Supporting Information

Chemical upcycling of Ni from electroplating wastewater to well-defined catalyst for electrooxidation of glycerol to formate

Ranran Zhai[a], Meiqi Zheng[a], Yifan Yan[a], Yue Ren[a], Zhenhua Li[a], Hua Zhou[a], Wenying Shi*[a,b], Xianggui Kong*[a,c], Mingfei Shao[a]

[a] State Key Laboratory of Chemical Resource Engineering, Beijing University of Chemical Technology, Beijing, 100029, China.

[b] Qingyuan Innovation Laboratory, Quanzhou, 362801, China

[c] Quzhou Institute for Innovation in Resource Chemical Engineering, Zhejiang, China

* Corresponding author:

E-mail: shiwy@buct.edu.cn (W. Shi); kongxg@buct.edu.cn (X. Kong)

Experiment section

Materials and reagents: Except noted, all chemicals were purchased and used without further purification. Deionized water was used throughout the experiments. potassium permanganate ($KMnO_4$), nickel sulfate ($NiSO_4$•$6H_2O$), potassium hydroxide (KOH), sodium hydroxide (NaOH), ethylenediamine tetraacetic acid disodium salt (EDTA) and Sodium hypophosphite (NaH_2PO_4•H_2O) were purchased from Sinopharm Chemical Reagent (Beijing Co., Ltd.). Glycerol ($C_3H_8O_3$, ≥99%) and oxalic acid, tartaric acid, pyruvic acid, glyceric acid, glycolic acid, lactic acid, formic acid, and acetic acid were obtained from Shanghai Macklin Biochemical Co., Ltd. All the above chemicals were used as received without further purification. Abbreviation: glycerol (GLY), oxalic acid (OA), tartaric acid (TA), pyruvic acid (PA) glyceric acid (GLA), glycolic acid (GA), lactic acid (LA), formic acid (FA) and acetic acid (AA)

The remediation performance to simulated Ni-electroplating solution: The effect of mole ratio of NaOH/Ni^{2+}: For example, firstly, 0.424 g NaH_2PO_4•H_2O was dissolved in 50 mL simulated Ni-electroplating solution to ensure the mole ratio of NaH_2PO_4/Ni^{2+} was 3. After that, 0.3 g NaOH was introduced into the above solution with vigorous stirring for 30 minutes. Then, the solution was transformed in a 100 mL Teflon-lined stainless-steel autoclave. After sealing the autoclave, it was heated to 160 °C for 6 h. After the reaction, the mixture solution (8 ml) was filtered through a 0.2-micron membrane filter, then the filtrates were analyzed using ICP-OES to detect the residual Ni^{2+} concentration. The precipitate was obtained by centrifugation and washed with deionized water and dried in oven. With the mole ratio of NaH_2PO_4/ Ni^{2+} kept constant, different amounts of NaOH were added to explore the effect to remove Ni^{2+} from solution.

The effect of mole ratio of NaH_2PO_4/Ni^{2+}: For example, firstly, 0.4 g NaOH was dissolved in 50 mL simulated Ni-electroplating solution to ensure the mole ratio of $NaOH/Ni^{2+}$ was 4. After that, 0.159 g $NaH_2PO_4 \cdot H_2O$ was introduced into the above solution with vigorous stirring for 30 minutes. Then, the solution was transformed in a 100 mL Teflon-lined stainless-steel autoclave. After sealing the autoclave, it was heated to 160 °C for 6 h. After the reaction, the mixture solution (8 ml) was filtered through a 0.2-micron membrane filter, then the filtrates were analyzed using ICP-OES to detect the residual Ni^{2+} concentration. The precipitate was obtained by centrifugation and washed with deionized water and dried in oven. With the mole ratio of $NaOH/Ni^{2+}$ kept constant, different amounts of $NaH_2PO_4 \cdot H_2O$ were added to explore the effect to remove Ni^{2+} from solution.

The remediation performance to actual Ni-electroplating solution: Firstly, 1.2 g NaOH and 1.5 g $NaH_2PO_4 \cdot H_2O$ were dissolved in 50 mL actual Ni-electroplating solution with vigorous stirring for 30 minutes. Then, the solution was transformed in a 100 mL Teflon-lined stainless-steel autoclave. After sealing the autoclave, it was heated to 160 °C for 6 h. After the reaction, the mixture solution (8 ml) was filtered through a 0.2-micron membrane filter, then the filtrates were analyzed using ICP-OES to detect the residual Ni^{2+} concentration. The precipitate was obtained by centrifugation and washed with deionized water and dried in oven.

Preparation of working electrode: The carbon cloth was firstly immersed in 0.5mol/L potassium permanganate solution for 30 min, then washed with deionized water and dried in a 60℃ oven. Mixed 16 mg electrocatalyst, 1.6 ml ethanol and 16 μL Nafion solution (5%, Macklin) together thoroughly, and ultrasonic for 30 min, after that, the mixture was deposited on the treated carbon cloth of 2*2.5 cm^2, and dried for 30 min.

Electrochemical measurement: All electrochemical measurements for glycerol oxidation were performed in 1 M KOH electrolyte at room temperature on an electrochemical workstation (CHI 760E, CH Instruments, Inc.). The electrochemical tests were performed in a three-electrode system in a membrane-free glass beaker, using Ag/AgCl electrode (with saturated KCl) and Pt foil as reference and counter electrode, respectively. Linear scan voltammetry (LSV) curves of catalysts were acquired from −0.2 V to 0.7 V vs. Ag/AgCl at a scan rate of 10 mV s^{-1}. All of the electrocatalytic reactions were conducted at ambient pressure and temperature, unless otherwise specified. All potentials measured against Ag/AgCl were converted to the reversible hydrogen electrode (RHE) scale using the following equations:

$$E_{\mathrm{RHE}} = E_{\mathrm{Ag/AgCl}} + E_{\mathrm{Ag/AgCl}\ vs.\ \mathrm{NHE}} + 0.059\ \mathrm{pH} \tag{1}$$

where $E_{\mathrm{Ag/AgCl}\ vs.\ \mathrm{NHE}}$ in eq (1) is 0.197 V at 20 °C.

The selectivity of the products was calculated based on total moles of GLY oxidation products using the following equations.

$$\mathrm{Selectivity} = \frac{n_{\mathrm{product}}}{n_{\mathrm{total}}} \times 100\% \tag{2}$$

The liquid products were quantified by high performance liquid chromatography (HPLC; Angilent 1200 Infinity Series) equipped with organic acid column (Coregel 87H3) using 5 mM aqueous H_2SO_4 as mobile phase and detected by UV detector (210 nm) and refractive index detector.

The product yield rate can be expressed using the following formula:

$$\text{Yield (mmol h}^{-1}\text{ g}^{-1}) = \frac{\text{Amount of product (mmol)}}{\text{Catalyst mass (g)} \times \text{Reaction time (h)}}$$

This formula can be adapted to express the yield of any product generated during the reaction, including formic acid or other products of glycerol oxidation.

Characterizations.

X-ray diffraction patterns were collected on a Shimadzu XRD-6000 diffractometer using a Cu Kα source, with a scan range of 5−80° and scan step of 10° min^{-1}. X-ray photoelectron spectra (XPS) were performed on a Thermo VG ESCALAB 250 X-ray photoelectron spectrometer at a pressure of about 2×10^{-9} Pa using Al Kα X-rays as the excitation source. Scanning electrode microscope (SEM) images were recorded by a Zeiss SUPRA 55 Field Emission SEM with an accelerating voltage of 20 kV. Transmission electron microscopy (TEM) images were recorded with JEOL JEM-2010 high resolution (HR-)TEM with an accelerating voltage of 200 kV. Metal contents in catalysts were determined by ICP-MS on a Thermo ICAP6300 Radial.

In situ Raman spectra were recorded on a confocal Raman microspectrometer (Renishaw, inVia-Reflex, 532 nm) using a 532 nm laser and the power was set at 2 mW under different potentials monitored by a CHI 760E electrochemical workstation equipped with an in situ Raman cell (Beijing Scistar Technology Co. Ltd). The applied potentials during the in situ Raman tests were not corrected by the solution resistance, which is constant with the LSV test without I-R correction (Fig. 4a), ensuring clear comparison of the results by using different techniques.

In situ FT-IR spectra were recorded by a Bruker Equinox 55 spectrometer, between 4000 and 400 cm−1 with a resolution of 4 cm−1 after 600 scans per spectrum. The electrochemical measurements were monitored by a CHI 760E electrochemical

108 workstation equipped with an in-situ FTIR cell (Beijing Scistar Technology Co. Ltd).
109 The FTIR cell is a three-electrode system, using Ag/AgCl electrode (with saturated
110 KCl) and Pt wire as reference and counter electrode, respectively. The working
111 electrode was prepared by loading S-C/Ni-P_x catalyst on glassy carbon electrode
112 (Figure S19). For the in-situ FTIR test, we first stabilized the catalyst in 1 M KOH at
113 1.6 V vs. RHE for 10 min, then 0.1 M GLY was added in the electrolyte and set this
114 time point as 0 min. The FTIR spectrum of S-C/Ni-P_x from 5 to 605s is shown in Figure
115 5d.

116

Supplementary Figures

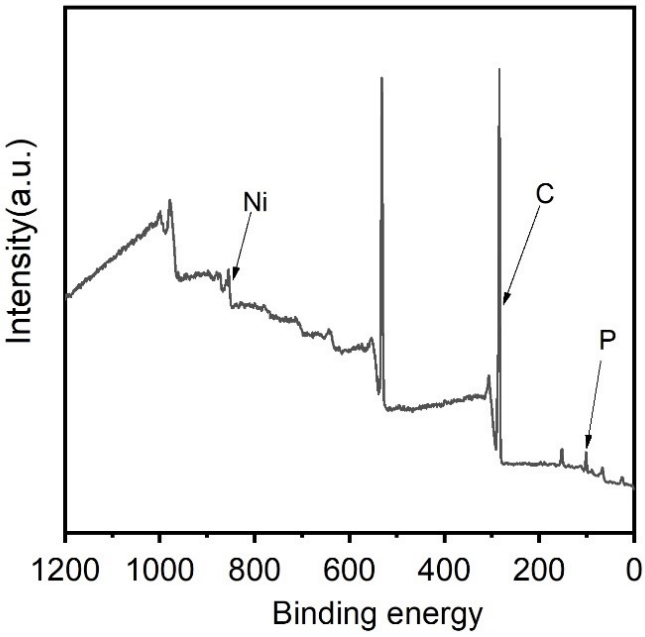

Figure S1. XPS survey spectra of the obtained precipitate from simulated Ni-electroplating solution

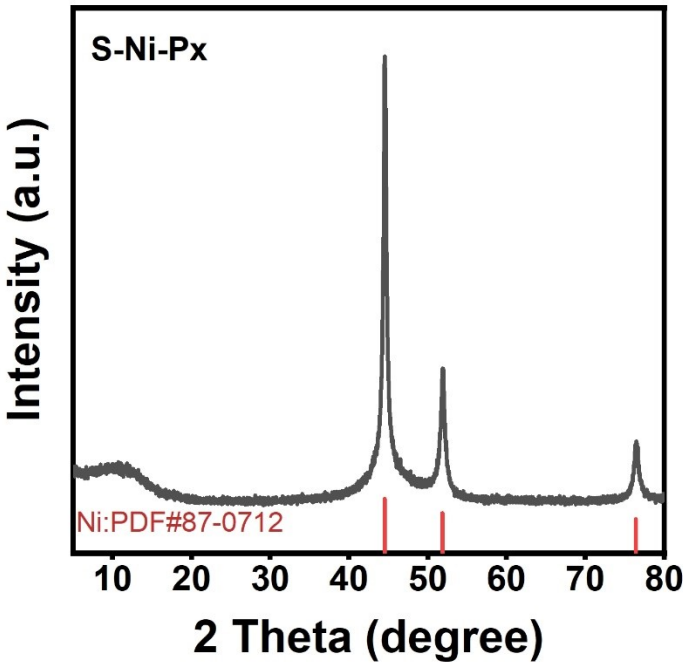

Figure S2. XRD patterns of the obtained precipitate

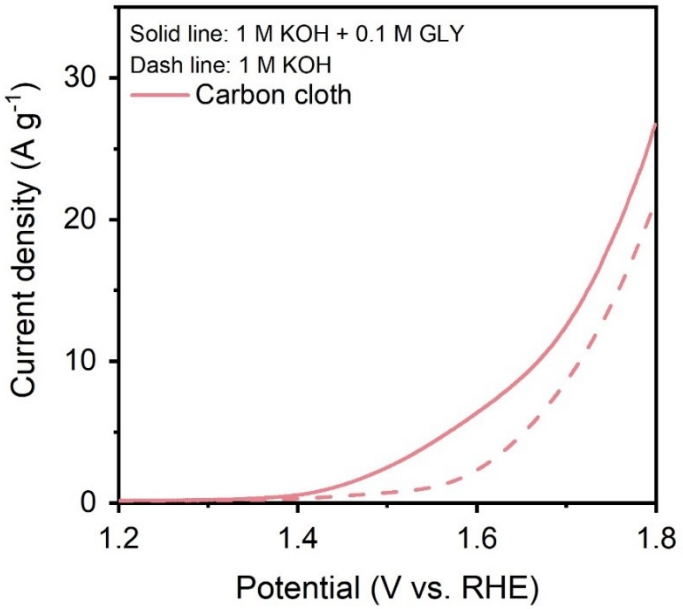

Figure S3. LSV curves of carbon cloth electrode at a scan rate of 10 mV/s in 1.0 M KOH with or without 0.1 M glycerol.

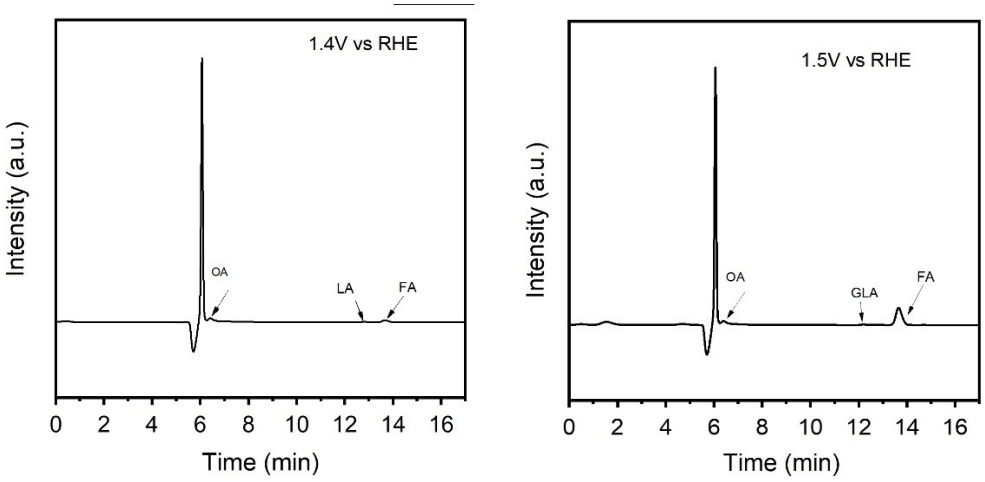

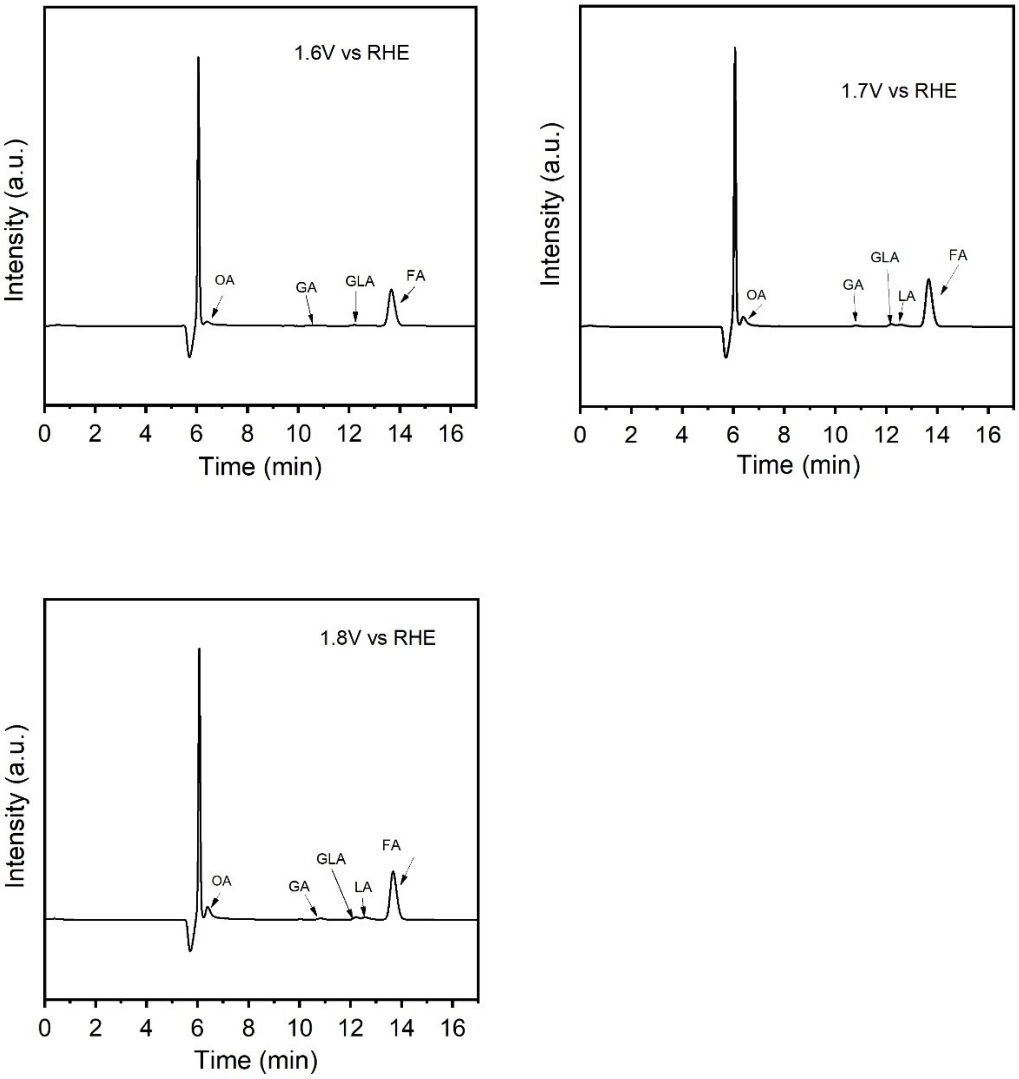

Figure S4. HPLC chromatogram of glycerol oxidation products over S-C/Ni-P_x at different potential.

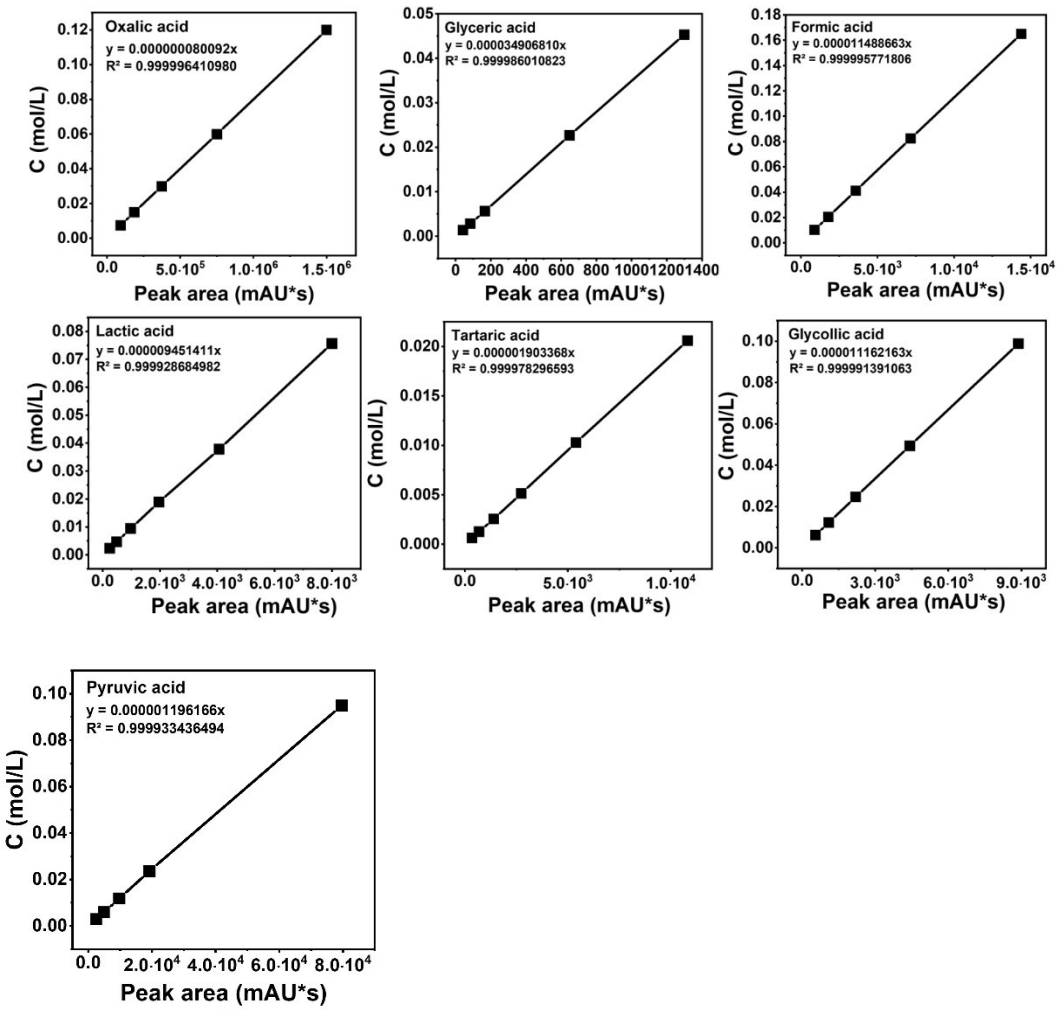

Figure S5. HPLC calibration curves of glycerol, reaction intermediates, and products with refractive index detector.

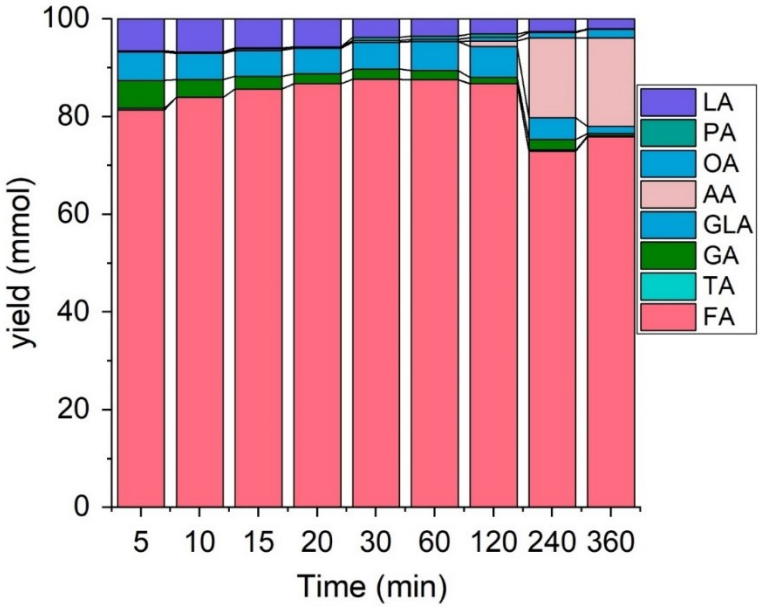

Figure S6. Yield of the detected products from glycerol electrooxidation versus the reaction time catalyzed by S-C/Ni-P_x.Reaction conditions: 1.0 M KOH with 0.1 M glycerol at 1.6 V vs. RHE.

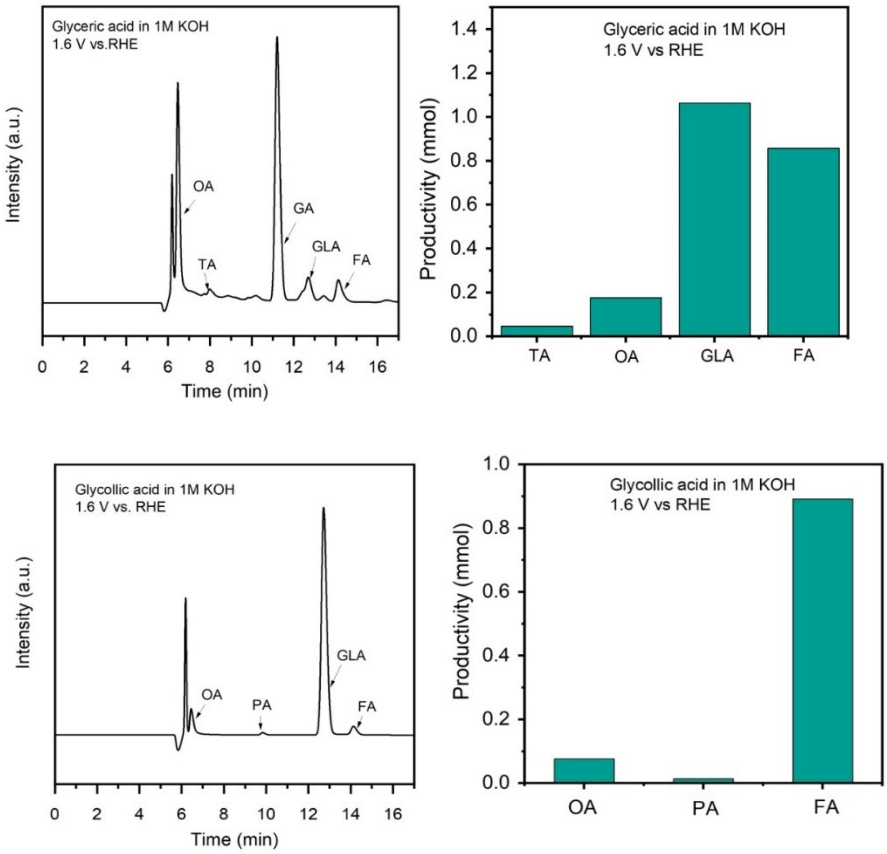

Figure S7. i-t experiments with glycerate and glycolate as substrates on S-C/Ni-Px catalyst were performed at the applied potential of 1.6 V vs RHE in 1 M KOH solution with 0.1 M of the

substrates.

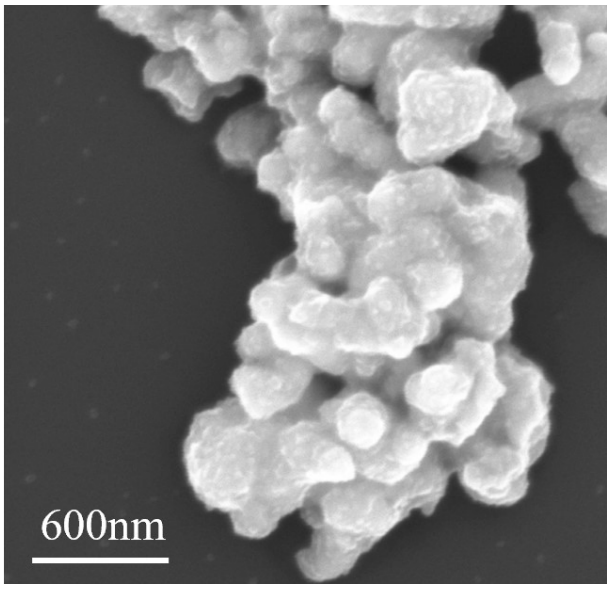

Figure S8. SEM image of the obtained precipitate

Supplementary Tables

Table S1. The main components and concentrations of simulated Ni-electroplating solution

Main components	Ni^{2+}	$H_2PO_2^-$	NH_4^+	$C_6H_5O_7^{3-}$	pH
Concentrations (mg/L)	3.0	4.5	9.0	2	4.8

Table S2. Comparison of Residual Nickel Concentrations and Compliance across Different Remediation Methods

Remediation Method	**Initial Nickel Concentration (mg/L)**	**Post-Treatment Nickel Concentration (mg/L)**	**Recovery of Ni^{2+} (%)**	**Ref.**
Sodium hypophosphite oxidation method	**3000**	**0.32**	**99.99**	**This work**
Two-Chamber Electrodeposition-Electrodialysis combination	325	\	82.34	1
RCE bench scale and RCE pilot plant reactors	1220	\	97	2
Solar Light Responsive Photocatalyst	8.1	1.5	81.48	3
integrated electrodeposition with adsorption pretreatment technique	53694.2	\	＞55	4
Electrocoagulation treatment processes	300	\	97	5
Chemical precipitation	\	0.003	99.88	6
Ion exchange	\	\	＞50	7

Comparison of processes and combined processes	\	\	99	8
extraction	500	\	90	9

Ministry of Environmental Protection of China. Discharge Standard of Pollutants for Electroplating (GB 21900-2008).

Table S3 The electroplating wastewater composition analysis

Main components	Ni^{2+}	$H_2PO_2^-$	NH_4^+	SO_4^{2-}	Cl^-	EDTA	pH
Concentrations (g/L)	8.7	30.8	0.2	1.2	3.4	4.6	5.5

Table S4. Comparisons of S-C/Ni-P_x with reported electrocatalysts to glycerol electrooxidation

Catalyst	**Electrolyte**	**Value-added products**	**Voltage (V)**	**Selectivity /FE**	**Ref.**
FeCoNi/C	0.1 M NaOH +0.1 M Glycerol	Formate	-	Sel. 34.1%	10
Bi-Co_3O_4	1.0 M KOH + 0.1 M Glycerol	Formate	1.223 1.297 1.446	Sel.97.01± 1.73%	11
$CuCo_2O_4$/CFC	1.0 M KOH + 0.1 M Glycerol	Formate	1.26	Sel. 80.6%	12
NixB	1.0 M KOH + 0.1 M Glycerol	Formate	1.535	Sel. 80%	13
CuNi/ ACF	0.1M KOH+0.1 M Glycerol	Formate	1.897	Sel.97.4%	14

CuCo-oxide	1.0 M KOH + 0.1 M Glycerol	Formate	1.31	Sel.62.9%	15
$Co_3(PO_4)_2$(CoP)	1.0 M KOH + 0.1 M Glycerol	Formate	1.33	Sel.82%	16
Pt-in-VGCC	1 M KOH + 0.6 M Glycerol	Formate	1.23	Sel.79%	17
Ni-Mo-N/CFC	1 M KOH + 0.1 M Glycerol	Formate	1.35	Sel.92.48%	18
$Ni(OH)_2$	1 M KOH + 0.1 M GlyceroL	Formate	1.65	Sel.81.3%	19
NiCrO-$V_{Cr,O}$	1 M KOH + 0.1 M Glycerol	Formate	1.37	Sel.98%	20
NiO	0.1 M KOH + 0.1 M GlyceroL	Formate	1.7	Sel.97%	21
C/Ni-P_x	**1.0 M KOH + 0.1 M Glycerol**	**Formate**	**1.6**	**Sel.96.4%**	**This work**

165

166

References

[1] K. Yan, P. Huang, M. Xia, X. Xie, L. Sun, W. Lei and F. Wang, Sep. *Purif. Technol*., 2022, **295**, 121283.

[2] F. J. Almazán-Ruiz, F. Caballero, M. R. Cruz-Díaz, E. P. Rivero, J. Vazquez-Arenas and I. González, *Chem. Eng. Res. Des*., 2015, **97**, 18–27.

[3] E.-C. Su, B.-S. Huang and M.-Y. Wey, *ACS Sustainable Chem. Eng*., 2017, **5**, 2146−2153.

[4] S. Li, M. Dai, I. Ali, H. Bian and C. Peng, *Process Saf. Environ. Prot*., 2023, **172**, 417–424.

[5] S. Vasudevan, J. Lakshmi, G. Sozhan, Environ. *Sci. Pollut. Res*., 2012, **19**, 2734–2744.

[6] Z. Mengesha Ayalew, X. Zhang, X. Guo, S. Ullah, S. Leng, X. Luo and N. Ma, Sep. *Purif. Technol*., 2020, **248**, 117114.

[7] A. Ma, A. Abushaikha, S. J. Allen and G. McKay, *Chem. Eng. J*., 2019, **358**, 1–10.

[8] A. Yasar, A. Ghaffar, Y. Mahfooz, A. B. Tabinda and A. Mehmood*, Desalination Water Treat*., 2021, **230**, 268–275.

[9] R. N. R. Sulaiman and N. Othman, *J. Environ. Chem. Eng*., 2018, **6**, 1814–1820.

[10] V.L. Oliveira, C. Morais, K. Servat, T.W. Napporn, G. Tremiliosi-Filho, K.B. Kokoh, Sep. *Purif. Technol*., 2014, **117**, 255-262.

[11] Y. Wang, Y.-Q. Zhu, Z. Xie, S.-M. Xu, M. Xu, Z. Li, L. Ma, R. Ge, H. Zhou, Z. Li, X. Kong, L. Zheng, J. Zhou, H. Duan, *ACS Catal*., 2022, **12**, 12432-12443.

[12] X. Han, H. Sheng, C. Yu, T.W. Walker, G.W. Huber, J. Qiu, S. Jin, *ACS Catal*., 2020, **10**, 6741-6752.

[13] S. Cychy, S. Lechler, Z. Huang, M. Braun, A.C. Brix, P. Blümler, C. Andronescu, F. Schmid, W. Schuhmann, M. Muhler, *Chinese J. Catal*., 2021, **42**, 2206-2215.

[14] J. Zhang, Y. Shen, *J. Electrochem. Soc*., 2021, **168**, 084510.

[15] L. Fan, Y. Ji, G. Wang, J. Chen, K. Chen, X. Liu, Z. Wen, *J. Am. Chem. Soc*., 2022, **144**, 7224-7235.

[16] I. Chauhan, P.M. Vijay, R. Ranjan, K.K. Patra, C.S. Gopinath, *ACS Mater. Au*., 2024, **4**, 500−511.

[17] S. Lee, H.J. Kim, E.J. Lim, Y. Kim, Y. Noh, G.W. Huber, W.B. Kim, *Green Chem*., 2016, **18**, 2877-2887.

[18] Y. Li, X. Wei, L. Chen, J. Shi, M. He, *Nat. Commun*., 2019, **10**.10.

[19] J. Wu, J. Li, Y. Li, X.Y. Ma, W.Y. Zhang, Y. Hao, W.B. Cai, Z.P. Liu, M. Gong, Angew. *Chem. Int. Ed*., 2022, **61**, e202113362.

[20] Z. Xia, C. Ma, Y. Fan, Y. Lu, Y.-C. Huang, Y. Pan, Y. Wu, Q. Luo, Y. He, C.-L. Dong, S. Wang, Y. Zou, *ACS Catal*., 2024, **14**, 1930-1938.

[21] J. Zhang, Y. Shen, H. Li, *ACS Appl. Energy Mater*., 2023, **6**, 5508-5518.